NEW HIGH ORDER UPWIND TECHNIQUES FOR ADVECTIVE TERM DISCRETIZATIONS

Rafael Alves Bonfim de Queiroz, bonfim@icmc.usp.br, bonfimraf@gmail.com
Fernando Akira Kurokawa, kurokawa@icmc.usp.br
Valdemir Garcia Ferreira, pvgf@icmc.usp.br
Departamento de Matemática Aplicada e Estatística do Instituto de Ciências Matemáticas e de Computação - SME-ICMC-USP; Av. Trabalhador São-Carlense, 400 - Centro; Caixa Postal: 668 - CEP: 13560-970 - São Carlos - SP; Fone: 55 (16) 3373-9700 - Fax: 55 (16) 3371-2238

Abstract. *In this work, two new high order upwind techniques for advective term discretizations are presented. The schemes are tested by solving the 1D inviscid Burgers equation and 2D incompressible Navier-Stokes equations. Two flows are simulated, namely: (i) a backward facing step; and (ii) a turbulent free jet impinging onto a rigid wall. The numerical results are compared with analytical and experimental data.*

Keywords: *high order upwind, convective transport, incompressible free-surface flow*

1. INTRODUCTION

The numerical solution of convection dominated PDE has been one of the most challenging problem in CFD research for the past three decades. And the success of the numerical simulation of these types of problems depends on the upwinding strategy for discretization of advective terms (in general, non linear). In the specialized literature, there exists a variety of schemes for approximating convection terms, but none of them has shown to be completely robust. In this context, the objective of this work is to present the development and application of two new bounded upwind schemes called ALUS (Adaptative Linear Upwind Scheme) (Queiroz and Ferreira, 2008) and TOPUS (Third-Order Polynomial Upwind Scheme) (Queiroz et al., 2008a; Queiroz et al., 2008b) for numerical solution of fluid dynamic problems. The derivation of these schemes is based on NVD (Normalized Variable Diagram) restrictions of Leonard (1988), and the TVD (Total Variation Diminishing) constraints of Harten (1983). Thus, they possess the boundedness property, i.e, they satisfy the CBC (Convection-Boundedness Criterion) of Gaskell and Lau (1988).

The performance of the ALUS and TOPUS schemes is investigated by using the 1D inviscid Burger equation and the 2D incompressible flows. For numerical simulation of flows, the full Navier-Stokes equations are solved by using the finite difference methodology on a staggered grid system, and the numerical procedure is an adaptation of the explicit SMAC (Simplified Marker-And-Cell) methodology of Amsden and Harlow (1970) for calculating free surface fluid flows at high Reynolds numbers. The calculations are performed using the 2D version of the Freeflow simulation system of Castelo et al. (2000). Numerical results compared with well know analytical and experimental data confirm the ability of the two new schemes.

The organization of this work is as follows. In Section 2, it is described the basic equations that model the flows and the numerical method. In Section 3, the mathematical formulation of the ALUS and TOPUS schemes is outlined. In Section 4, 1D test case and 2D numerical examples are performed for the verification/validation of these modern techniques for advective term discretizations. Conclusions are presented in Section 5.

2. BASIC EQUATIONS AND THE NUMERICAL METHOD

2.1 1D Inviscid Burgers equation

The inviscid Burgers equation is given by

$$u_t + \left(\frac{u^2}{2}\right)_x = 0. \tag{1}$$

2.2 Full Navier-Stokes equations

The general mathematical equations that model transient Newtonian incompressible flows are Navier-Stokes and mass conservation equations, respectively, that is

$$\frac{\partial \mathbf{u}}{\partial t} + \nabla \cdot (\mathbf{uu}) = -\nabla p + \frac{1}{Re}\nabla^2 \mathbf{u} + \frac{1}{Fr^2}\mathbf{g}, \tag{2}$$

$$\nabla \cdot \mathbf{u} = 0, \tag{3}$$

where the velocity $\mathbf{u}$ is the vector consisting of the velocity components, the pressure p is a scalar, and $\mathbf{g}$ is the gravitational acceleration ($|\mathbf{g}| = 9,81$ m/s^2). The non-dimensional parameters $Re = (LU)/\nu$ and $Fr = U/(\sqrt{L|\mathbf{g}|})$ are, respectively, the Reynolds and Froude numbers, in which L is length scale and U is characteristic velocity. ν is kinematic viscosity coefficient (constant) of the fluid. Together with appropriate boundary and initial conditions, the Eqs. (2) and (3) are solved by using the finite difference method implemented in the 2D version of the Freeflow code of Castelo et al. (2000). This code uses an explicit version of the SMAC method originally proposed by Amsden and Harlow (1970). The details of the discretization procedure have been presented by Ferreira et al. (2004, 2007).

2.3 Initial and boundary conditions

Equations (2) and (3) are coupled non-linear PDEs and are sufficient, in principle, to solve for the unknowns $\mathbf{u}$ and p when appropriate initial and boundary conditions are specified. For initial conditions, a Dirichlet condition is used for all variables. There are four types of boundaries to be considered, namely: inlet, outlet, solid walls and free surfaces. At the inlet section, the velocity is known. At the outlet section, homogeneous Neumann (fully developed flow) conditions are specified for all variables. On the solid walls, it is assumed that the fluid adheres to (no slip) or slips at (free slip) the solid surface. The appropriate free-surface boundary conditions are the vanishing of the normal and tangential stresses which, in the absence of surface tension, are (see Ferreira et al. (2004, 2007) for details)

$$\mathbf{n} \cdot \mathbf{T} \cdot \mathbf{n} = 0, \tag{4}$$

$$\mathbf{m} \cdot \mathbf{T} \cdot \mathbf{n} = 0, \tag{5}$$

where $\mathbf{n}$ is the local unit normal vector, external to the free surface, and $\mathbf{m}$ is the local tangent vector to the free surface. The viscous stress tensor $\mathbf{T}$ is given by

$$\mathbf{T} = -p\mathbf{I} + 2\mu\mathbf{D}, \tag{6}$$

where $\mathbf{I}$ is identity tensor, μ is dynamic viscosity coefficient, and $\mathbf{D}$ is tensor of deformations average

$$\mathbf{D} = 0.5\left(\nabla\mathbf{u} + (\nabla\mathbf{u})^T\right). \tag{7}$$

2.4 Numerical method

The PDEs (2) and (3) have been solved numerically by using the staggered grid finite difference methodology, presented by Tomé et al. (2000). An important factor in the choice of the spatial differencing strategy, a topic of this study, is the order of accuracy. In the present study, the diffusion terms have been approximated by second order central differencing, while for the advection terms by the ALUS and TOPUS schemes. Details of these schemes will be presented in the next subsection. The Poisson equation (see Eq. (12)) is discretized using the usual five-point Laplacian operator, and the associated symmetric linear system is solved by the conjugate-gradient method. The complete numerical algorithm is summarized below.

When calculating the tilde velocity, $\tilde{\mathbf{u}}$, it is employed an adaptive time stepping procedure to compute the maximum permissible time step.

In this work, the Eqs. (2) and (3) are discretized in time by using the explicit Euler method, giving the system

$$\mathbf{u}^{(n+1)} = \mathbf{u}^{(n)} + \delta t\left\{-\nabla\cdot(\mathbf{uu})^{(n)} - \nabla p^{(n)} + \frac{1}{Re}\nabla^2\mathbf{u}^{(n)} + \frac{1}{Fr^2}\mathbf{g}^{(n)}\right\}, \tag{8}$$

$$\nabla\cdot\mathbf{u}^{(n)} = 0, \tag{9}$$

where δt is the time step. The solution procedure for solving Eqs. (8) and (9) can be accomplished by means of the fractional step procedures, first suggested by Chorin (1968), called projection methods. The basic idea behind this approach is to use the Eq. (8) to solve for an intermediate velocity field $\tilde{\mathbf{u}}$ that is not required to be divergence-free, that is,

$$\tilde{\mathbf{u}} = \mathbf{u}^{(n)} + \delta t\left\{-\nabla\cdot(\mathbf{uu})^{(n)} - \nabla\tilde{p} + \frac{1}{Re}\nabla^2\tilde{\mathbf{u}} + \frac{1}{Fr^2}\mathbf{g}^{(n)}\right\}, \tag{10}$$

where $\tilde{p} = p^{(n)}$ is a tentative pressure. Then, using Helmholtz-Hodge theory (Denaro, 2003), this intermediate velocity vector field is projected to ensure mass balance and obtain a gradient field ψ, that is,

$$\tilde{\mathbf{u}} = \mathbf{u}^{(n)} + \nabla\psi. \tag{11}$$

By applying the divergence in Eq. (11) and using Eq. (9), one obtain the following Poisson equation for ψ

$$\nabla^2\psi = \nabla\cdot\tilde{\mathbf{u}}. \tag{12}$$

For the computational approach, it is supposed that, at a given time $t = t_0$, the solenoidal-velocity field $\mathbf{u}(\mathbf{x}, t_0)$ is known and suitable boundary conditions for the velocity and pressure are given. The updated velocity field $\mathbf{u}(\mathbf{x}, t)$, at $t = t_0 + \delta t$, is calculated by the following sequence of the steps:

STEP 1: Update the variables on the boundaries: the conditions on inlets, outlets and rigid walls are discussed in subsection 2.3; in the case 2D, the velocity field at the free surface is explicitly computated using the following equations

$$\frac{1}{Re}\left[2\frac{\partial u}{\partial x}n_x m_x + 2\frac{\partial v}{\partial y}n_y m_y + \left(\frac{\partial u}{\partial y} + \frac{\partial v}{\partial x}\right)(n_y m_x + n_x m_y)\right] = 0, \tag{13}$$

where $\mathbf{n} = (n_x, n_y)$ is the local unit normal vector, external to the free surface, and $\mathbf{m} = (m_x, m_y)$ is the local tangent vector to the free surface. The pressure field is explicitly computed using the following equation

$$-p + \frac{2}{Re}\left[\frac{\partial u}{\partial x}n_x^2 + \frac{\partial v}{\partial y}n_y^2 + \left(\frac{\partial u}{\partial y} + \frac{\partial v}{\partial x}\right)n_x n_y\right] = 0; \tag{14}$$

STEP 2: Calculate the auxiliary velocity field from Eq. (10);

STEP 3: Solve the Poisson Eq. (12) for potential function ψ. The appropriate boundary conditions for this equation are homogeneous Dirichlet-type on the outlets and homogeneous Neumann-type on the fixed boundaries and inlets;

STEP 4: Compute the velocity field from (11);

STEP 5: Compute the pressure. It can be shown that the pressure is given by

$$p(\mathbf{x}, t) = \tilde{p}(\mathbf{x}, t) + \frac{\psi(\mathbf{x}, t)}{\delta t}; \tag{15}$$

STEP 6: Update the positions of the marker particles. This step involves moving the marker particles to their new positions. These are virtual particles (without mass, volume, or other properties), whose coordinates are stored and updated at the end of each computational cycle by solving the ordinary differential equation $\dot{\mathbf{x}} = \mathbf{v}$ by Euler's method. This provides a discrete particle, convected in a Lagrangian manner, with its new coordinates, allowing us to determine whether or not it has moved into a new computational cell, or if it has left the containment region through an outlet boundary. And go back to the **STEP 1**.

3. NEW SCHEMES FOR CONVECTIVE TERMS DISCRETIZATION

3.1 Introduction to normalized variables

Let $\phi(x, y)$ be the variation of one scalar in the normal direction to a f face, as shown in Fig. 1. In this figure, D (*Downstream*), U (*Upstream*) and R (*Remote-Upstream*) positions (see Ferreira et al., 2008) are determined with respect the convecting velocity at the f interface (flow direction). In order to facilitate the analysis of the functional relationship

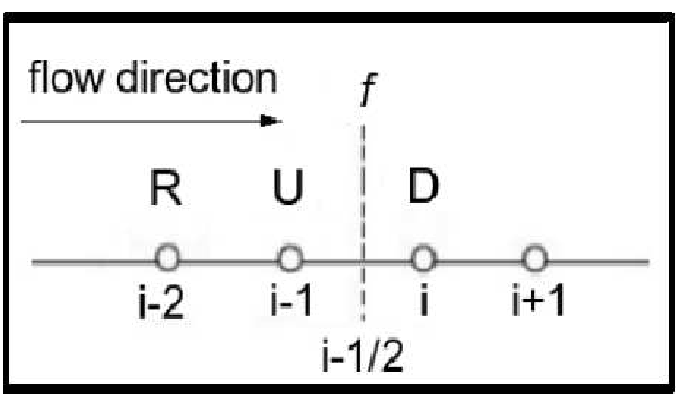

Figure 1. Computational stencil.

linking ϕ_D, ϕ_U and ϕ_R, the original variables are transformed in normalized variables (NV) of Leonard (1988) as

$$\hat{\phi} = \frac{\phi - \phi_R}{\phi_D - \phi_R}. \tag{16}$$

3.2 ALUS scheme

The ALUS scheme (Queiroz and Ferreira, 2008) is defined in NV as

$$\hat{\phi}_f = \begin{cases} 2\hat{\phi}_U, & \hat{\phi}_U \in (0, \lambda_a], \\ (1-0.5\beta)\hat{\phi}_U + 0.5\beta, & \hat{\phi}_U \in (\lambda_a, 1), \\ \hat{\phi}_U, & \hat{\phi}_U \notin (0,1), \end{cases} \tag{17}$$

where $\beta \in [0,1]$ and $\hat{\phi}_U = \frac{\phi_U - \phi_R}{\phi_D - \phi_R}$. Although $\beta \in [0,1]$ guarantees that the ALUS is convergent (see Fig. 2). In general, it is suggested to reader to use $\beta \in [0, 0.5]$ for flows with high Reynolds number (in order to ensure stability of the method). The adaptative variable λ_a in Eq. (17) is the intersection of $(1-0.5\beta)\hat{\phi}_U + 0.5\beta$ and $2\hat{\phi}_U$, whose result is

$$\lambda_a = \frac{0.5\beta}{1+0.5\beta}. \tag{18}$$

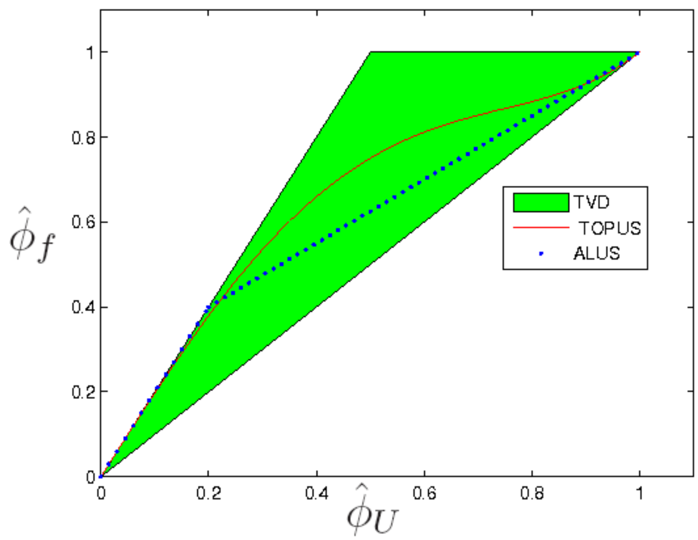

Figure 2. Upwind schemes in the TVD region: (a) ALUS-$\beta = 0.5$, (b)TOPUS-$\alpha = 2$.

In original variables, the ALUS scheme is given by

$$\phi_f = \begin{cases} 2\phi_U - \phi_R, & \hat{\phi}_U \in (0, \lambda_a], \\ (1-0.5\beta)\phi_U + 0.5\beta\phi_D & \hat{\phi}_U \in (\lambda_a, 1), \\ \phi_U, & \hat{\phi}_U \notin (0,1). \end{cases} \tag{19}$$

3.3 TOPUS scheme

The TOPUS scheme (see Queiroz et al. (2008a) and Queiroz et al. (2008b)) is defined in NV as

$$\hat{\phi}_f = \begin{cases} \alpha\hat{\phi}_U^4 + (-2\alpha+1)\,\hat{\phi}_U^3 + \left(\frac{5\alpha-10}{4}\right)\hat{\phi}_U^2 + \left(\frac{-\alpha+10}{4}\right)\hat{\phi}_U, & \hat{\phi}_U \in [0,1]; \\ \hat{\phi}_U, & \hat{\phi}_U \notin [0,1]; \end{cases} \tag{20}$$

where $\alpha \in [-2, 2]$ ensures that the scheme satisfies the CBC criterion (bounded solution). It is advisable to choose $\alpha = 2$, because it ensures that the TOPUS belongs to the class of the TVD schemes (see Fig. 2). In original variables, this scheme can be rewritten as

$$\phi_f = \begin{cases} \phi_R + (\phi_D - \phi_R)\left[\alpha\hat{\phi}_U^4 + (-2\alpha+1)\,\hat{\phi}_U^3 + \left(\frac{5\alpha-10}{4}\right)\hat{\phi}_U^2 + \left(\frac{-\alpha+10}{4}\right)\hat{\phi}_U\right], & \hat{\phi}_U \in [0,1]; \\ \phi_U, & \hat{\phi}_U \notin [0,1]; \end{cases} \tag{21}$$

For the spatial advection terms of Navier-Stokes equations, the application of this scheme is as follow. For simplicity, only the discretization of the nonlinear terms in u-component of Eq. (2) will be presented. The discretization of the other nonlinear term is made in a similar manner. In position $(i+\frac{1}{2},j)$ of the 2D mesh, this term can be approximated by the following conservative scheme (in this example, the f face corresponds to the $i+\frac{1}{2}$ in Fig. 1):

$$\left(\frac{\partial(uu)}{\partial x}+\frac{\partial(uv)}{\partial y}\right)\bigg|_{i+\frac{1}{2},j} \approx \frac{\bar{u}_{i+1,j}u_{i+1,j}-\bar{u}_{i,j}u_{i,j}}{\delta x} + \frac{\bar{v}_{i+\frac{1}{2},j+\frac{1}{2}}u_{i+\frac{1}{2},j+\frac{1}{2}}-\bar{v}_{i+\frac{1}{2},j-\frac{1}{2}}u_{i+\frac{1}{2},j-\frac{1}{2}}}{\delta y},$$

where the advection velocities $\bar{u}_{i+1,j}$, $\bar{u}_{i,j}$, $\bar{v}_{i+\frac{1}{2},j+\frac{1}{2}}$ and $\bar{v}_{i+\frac{1}{2},j-\frac{1}{2}}$ are obtained by averaging.

For instance, $\bar{v}_{i+\frac{1}{2},j-\frac{1}{2}}$ is approximate by

$$\bar{v}_{i+\frac{1}{2},j-\frac{1}{2}} \approx 0.5\left(v_{i,j-\frac{1}{2}}+v_{i+1,j-\frac{1}{2}}\right). \tag{22}$$

The velocities $u_{i,j}$ and $u_{i+1,j}$ are calculated (the other velocities follow similar procedures) for example using the TOPUS scheme by the conditions:

- If $\bar{u}_{i,j}>0$ and $\hat{u}_{i-\frac{1}{2},j}=\frac{u_{i-\frac{1}{2},j}-u_{i-\frac{3}{2},j}}{u_{i+\frac{1}{2},j}-u_{i-\frac{3}{2},j}}$, then

$$u_{i,j,k}=\begin{cases} u_{i-\frac{3}{2},j}+(u_{i+\frac{1}{2},j}-u_{i-\frac{3}{2},j})\left[2\hat{u}^4_{i-\frac{1}{2},j}-3\hat{u}^3_{i-\frac{1}{2},j}+2\hat{u}_{i-\frac{1}{2},j}\right], & \hat{u}_{i-\frac{1}{2},j}\in[0,1];\\ u_{i-\frac{1}{2},j}, & \hat{u}_{i-\frac{1}{2},j}\notin[0,1]; \end{cases}$$

- If $\bar{u}_{i,j}<0$ and $\hat{u}_{i+\frac{1}{2},j}=\frac{u_{i+\frac{1}{2},j}-u_{i+\frac{3}{2},j}}{u_{i-\frac{1}{2},j}-u_{i+\frac{3}{2},j}}$, then

$$u_{i,j}=\begin{cases} u_{i+\frac{3}{2},j}+(u_{i-\frac{1}{2},j}-u_{i+\frac{3}{2},j})\left[2\hat{u}^4_{i+\frac{1}{2},j}-3\hat{u}^3_{i+\frac{1}{2},j}+2\hat{u}_{i+\frac{1}{2},j}\right], & \hat{u}_{i+\frac{1}{2},j}\in[0,1];\\ u_{i+\frac{1}{2},j}, & \hat{u}_{i+\frac{1}{2},j}\notin[0,1]; \end{cases}$$

- If $\bar{u}_{i+1,j}>0$ and $\hat{u}_{i+\frac{1}{2},j}=\frac{u_{i+\frac{1}{2},j}-u_{i-\frac{1}{2},j}}{u_{i+\frac{3}{2},j}-u_{i-\frac{1}{2},j}}$, then

$$u_{i+1,j}=\begin{cases} u_{i-\frac{1}{2},j}+(u_{i+\frac{3}{2},j}-u_{i-\frac{1}{2},j})\left[2\hat{u}^4_{i+\frac{1}{2},j}-3\hat{u}^3_{i+\frac{1}{2},j}+2\hat{u}_{i+\frac{1}{2},j}\right], & \hat{u}_{i+\frac{1}{2},j}\in[0,1];\\ u_{i+\frac{1}{2},j}, & \hat{u}_{i+\frac{1}{2},j}\notin[0,1]; \end{cases}$$

- If $\bar{u}_{i+1,j}<0$ and $\hat{u}_{i+\frac{3}{2},j}=\frac{u_{i+\frac{3}{2},j}-u_{i+\frac{5}{2},j}}{u_{i+\frac{1}{2},j}-u_{i+\frac{5}{2},j}}$, then

$$u_{i+1,j}=\begin{cases} u_{i+\frac{5}{2},j}+(u_{i+\frac{1}{2},j}-u_{i+\frac{5}{2},j})\left[2\hat{u}^4_{i+\frac{3}{2},j}-3\hat{u}^3_{i+\frac{3}{2},j}+2\hat{u}_{i+\frac{3}{2},j}\right], & \hat{u}_{i+\frac{3}{2},j}\in[0,1];\\ u_{i+\frac{3}{2},j}, & \hat{u}_{i+\frac{3}{2},j}\notin[0,1]. \end{cases}$$

4. NUMERICAL EXPERIMENTS

4.1 1D Inviscid Burgers equation

In this study, it is investigated the inviscid Burgers equation defined by Eq. (1) with initial condition (see Ahmed (2004)) defined as

$$u(0,t)=\begin{cases} 0, & x<-1;\\ 0.5, & -1<x<0;\\ 0, & x>0. \end{cases} \tag{23}$$

The exact solution for this Riemann problem for $t<4$ is given by (see Ahmed (2004))

$$u(x,t)=\begin{cases} 0, & x<-1;\\ \frac{x+1}{t}, & -1<x<\frac{t}{2}-1;\\ 0.5, & \frac{t}{2}-1<x<\frac{t}{4};\\ 0, & \frac{t}{4}<x. \end{cases} \tag{24}$$

In this test, it is considered a mesh size of $N=200$ computational cells ($\delta x=0.0125$), final time $t=2$, and $x\in[-1,1]$. The numerical results obtained using the ALUS-$\beta=0.95$ and TOPUS-$\alpha=2$ schemes and the exact solution are presented in Figs. 3 and 4, respectively. One can see from these figures that the solutions obtained by the two schemes are better when one uses time step $\delta t=0.01625$. Besides, these figures show a satisfactory concordance between the numerical and analytical data.

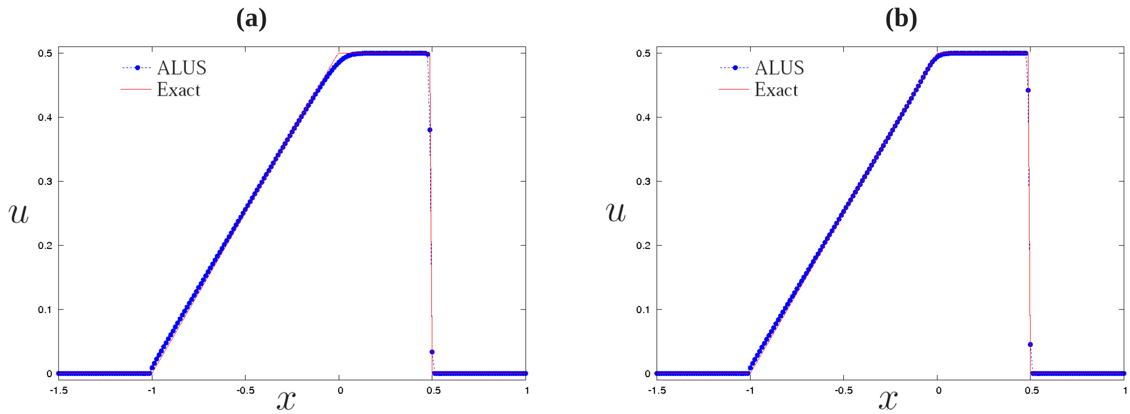

Figure 3. Comparison between numerical result by using ALUS and exact solution: **(a)** $\delta t = 0.01125$; **(b)** $\delta t = 0.01625$.

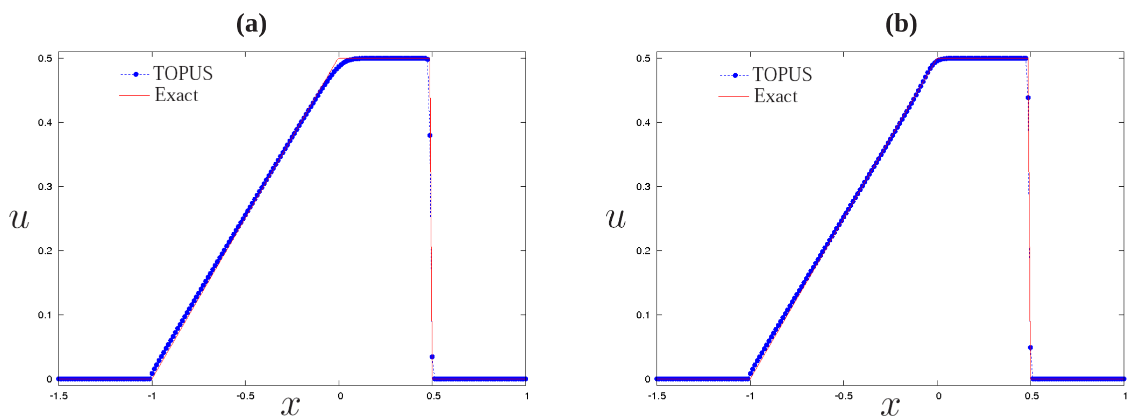

Figure 4. Comparison between numerical result by using TOPUS and exact solution: **(a)** $\delta t = 0.01125$; **(b)** $\delta t = 0.01625$.

4.2 2D Backward facing step

The geometry for this 2D problem is illustrated in Fig. 5. The Freeflow code run this problem at Reynolds number 400, which was based on the following scaling parameters, namely: maximum velocity $U_{max} = 1.0$ m/s; and inlet diameter $L = 0.1$ m. The data for the numerical experiment were: 400×20 ($\delta_x = \delta_y = 0.1$ m) computational cells; dimension of domain 4.0 m $\times$ 0.2 m; and simulation time 100s. The experimental result of Armaly (1983) for the non-dimensional reattachment x_1 (see Fig. 5) 8.72 was used for comparison. The numerical results obtained by the ALUS-$\beta = 0.95$ and TOPUS-$\alpha = 2$ schemes are, respectively, 8.40 and 8.30, which are in a good agreement with the experimental result of Armaly and other data of the literature.

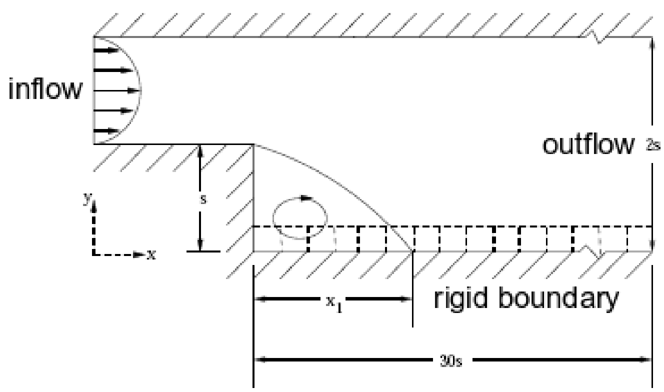

Figure 5. Geometry of the backward facing step problem.

(a)

(b)

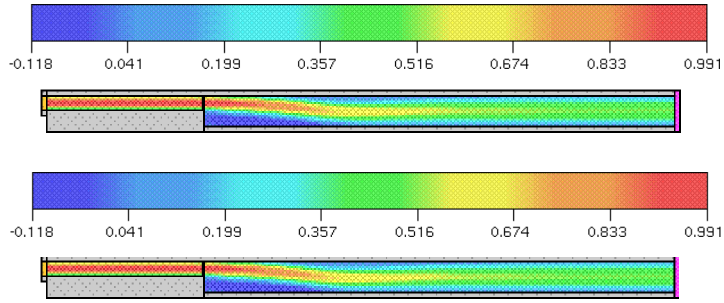

Figure 6. Numerical solution obtained for the component velocity u by using: **(a)** ALUS-$\beta = 0.95$; **(b)** TOPUS-$\alpha = 2$.

4.3 2D turbulent free jet impinging onto a rigid wall

A 2D jet impinging normally onto flat surface at high Reynolds number is a very important test case for assessing the performance of convection terms discretization. In turbulent regime, this free surface flow has been chosen as a representative test bed because there is (see Watson (1964)) an approximated analytical solution for the total thickness of the fluid layer flowing on a flat rigid wall. This problem is difficult to simulate because the free surface boundary conditions must be specified on an arbitrarily moving boundary (see an illustration in Fig. 7). The Freeflow code run this

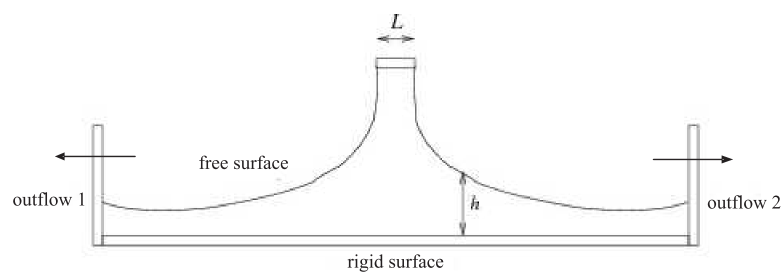

Figure 7. Configuration of a free jet impinging onto a rigid surface.

problem at Reynolds number of 5.0×10^4, which was based on the maximum velocity $U_{max} = 1.0$ m/s and diameter of the inlet $L = 0.01$ m. Three meshes were used, namely: the coarse 200×50 ($\delta_x = \delta_y = 0.001$ m); the medium 400×100 ($\delta_x = \delta_y = 0.0005$ m); and the fine 800×200 ($\delta_x = \delta_y = 0.00025$ m) computational cells. By using these meshes, a comparison was made between the free surface height (the total thickness of the layer), obtained from numerical methods (ALUS-$\beta = 0.4$ and TOPUS-$\alpha = 2$ and the analytical viscous solution of Watson (1964). This is displayed in Figs. 8 (a) and (b). One can see from these figures that the numerical results on fine mesh are generally in good agreement with the analytical solution, displaying small differences in some regions of the flow.

(a) **(b)**

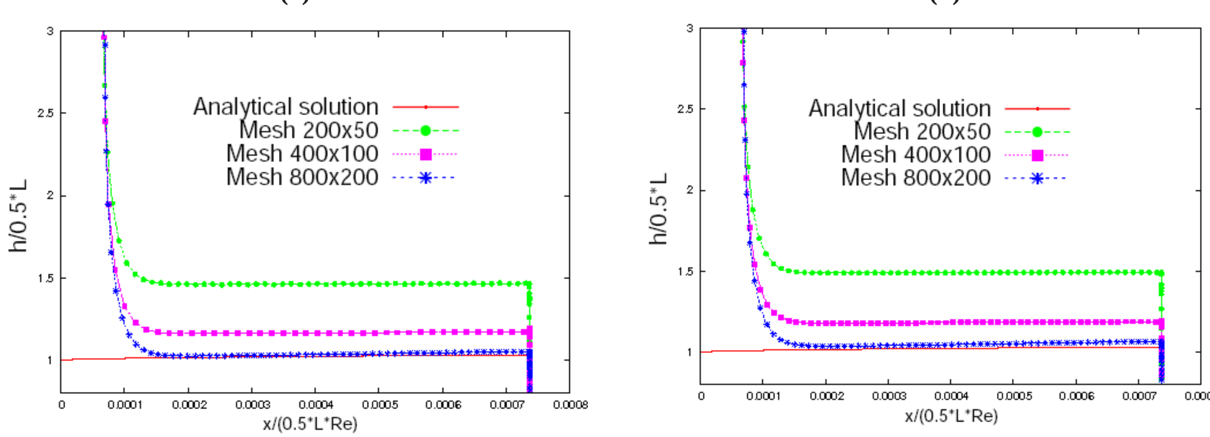

Figure 8. Comparison on three meshes between numerical solution and analytical solution of Watson (1964): **(a)** ALUS-$\beta = 0.4$; **(b)** TOPUS-$\alpha = 2$.

5. CONCLUSION

In this work, two new high order upwind schemes for advective term discretizations (called ALUS and TOPUS) have been proposed. In the 1D/2D numerical experiments here investigated, both schemes provided good results when compared with analytical solution and experimental data. For the future, the authors will be concerned with to the application of theses high order upwind techniques for solving non-Newtonian and turbulent flows.

6. ACKNOWLEDGEMENTS

This research work was supported by the *FAPESP* under Grants 04/16064-9, 05/51458-0, 06/05910-1 and *CNPq* under Grant 304201/05-7.

7. REFERENCES

Ahmed, R., 2004, “Numerical Schemes Applied to the Burgers and Buckley-Leverett Equations”, Msc dissertation, University of Reading.

Amsden, A.A. and Harlow, F.H., 1970, “A simplified MAC technique for incompressible fluid flow calculations”, Journal of Computational Physics, Vol. 6, pp. 322.

Armaly, B.F., Durst, F., Periera, J.C.F. and Schonung, B., 1983, “Experimental and theoretical investigation of backward facing step flow”, Journal of Fluid Mechanics, Vol. 127, pp. 473.

Castelo, A., Tomé, M.F., McKee, S., Cuminato, J.A. and Cesar, C.N.L., 2000, “Freeflow: an integrated simulation system for three-dimensional free surface flows”, Comput. Visualization in Science, Vol. 2, pp. 1-12.

Chorin, A., 1968, “Numerical solution of the Navier-Stokes equations”, Mathematics of Computation, Vol. 22, pp. 745-762.

Denaro, F.M., 2003, “On the applications of the Helmholtz-Hodge decomposition in projection methods for incompressible flows with general boundary conditions”, International Journal for Numerical Methods in Fluids, Vol. 43, pp. 43-69.

Ferreira, V.G., Mangiavacchi, N., Tomé, M.F., Castelo, A., Cuminato, J.A. and Mckee, S., 2004, “Numerical simulation of turbulent free surface flow with two-equation k-e eddy-viscosity models”, International Journal for Numerical Methods in Fluids, Vol. 44, pp. 347-375.

Ferreira, V.G., Oishi, C.M., Kurokawa, F.A., Kaibara, M.K., Cuminato, J.A, Castelo, A., Mangiavacchi, N., Tomé, M.F. and McKee, S., 2007, “A combination of implicit and adaptative upwind tools for the numerical solution of incompressible free surface flows”, Communication in Numerical Methods in Engineering, Vol. 23, pp. 419-445.

Ferreira, V.G., Kurokawa, F.A., Queiroz, R.A.B, Kaibara, M.K., Oishi, C.M, Cuminato, J.A, Castelo, A., Tomé, M.F. and Mckee, S., 2008, “An Assessment of a high-order finite difference upwind scheme for the simulation of convection-diffusion problems”, International Journal for Numerical Methods in Fluids, In Press.

Gaskell, P.H. and Lau, A.K.C., 1988, “Curvature-compensated convective transport: SMART, a new boundedness-preserving transport algorithm”, International Journal for Numerical Methods in Fluids, Vol. 8, pp. 617-641.

Harten, A., 1983, “High resolution schemes for conservation laws”, Journal of Computational Physics, Vol. 49, pp. 357-393.

Leonard, B.P., 1988, “Simple high-accuracy resolution program for convective modeling of discontinuities”, International Journal for Numerical Methods in Fluids, Vol. 8, pp. 1291-1318.

Queiroz, R.A.B. and Ferreira, V.G., 2008, “A new upwind scheme for numerical solution of fluid dynamics problems”, Anais do I Encontro Regional de Matemática Aplicada e Computacional-ERMAC, Bauru-SP.

Queiroz, R.A.B., Cuenca, R.G., Ferreira, V.G. and Souza, L.F., 2008a, “A new high resolution TVD scheme for unsteady flows with shock waves”, Proceedings of the 7th Brazilian Conference On Dynamics, Control and Applications - DINCON 2008, Presidente Prudente-SP.

Queiroz, R.A.B., Kurokawa, F.A. and Ferreira, V.G., 2008b, “Development and implementation of polynomial scheme for the numerical solution of 1D conservation laws”, Anais do VIII Simpósio Mecânica Computacional-SIMMEC, Belo Horizonte-MG.

Tomé, M.F., Castelo, A., Murakami, J., Cuminato, J. A., Minghim, R., Oliveira, M.C.F, Mangiavacchi, N. and Mckee, S., 2000, “Numerical simulation of axisymmetric free surface flows”, Journal of Computational Physics, Vol. 157, pp. 441-472.

Watson, E.J., 1964, “The radial spread of a liquid jet over a horizontal plane”, Journal of Fluid Mechanics, Vol. 20, pp. 481-499.

8. Responsibility notice

The authors are the only responsible for the printed material included in this paper.